DOI : 10.5958/2277-8934.2015.00021.1 *Vol 22 No 1, p 133-139*

ADVANCED IMAGING STUDIES ON NORMAL STIFLE JOINT OF CAMEL (*Camelus dromedarius*)

A. Sangwan and T.K. Gahlot

Department of Veterinary Surgery and Radiology, College of Veterinary and Animal Science, Rajasthan University of Veterinary and Animal Sciences, Bikaner 334001, India

ABSTRACT

Computed radiography and computed tomographic scanning of normal stifle joint of camel obtained from cadaver were studied and compared. The radiography revealed only the bony structures involved in the joint whereas CT scan revealed both bony and soft tissues. Lateral, cranio-caudal and caudo-cranial radiographs were taken which revealed all bones and articular surfaces of stifle joint. CT scan studies were done on 3-D, transverse and sagittal sections. Medial patellar ligament was not evidenced, however, the medial femoro-patellar ligament was distinguishable. Other important anatomical structures evident were cranial and caudal cruciate ligament, medial collateral ligament, lateral patellar retinaculum, middle patellar ligament, attachments of lateral and medial menisci and most of the associated muscles around stifle joint. CT scan also revealed the bony structures of the joint i.e. femoral trochlea, femoral condyles, tibial condyles, intercondylar tubercles, patella, tibial tuberosity etc.

Key words: Camel, computed radiograph, CT scan and stifle joint

The stifle joint is a modified hinge joint that must allow flexion and rotation, yet provide complete stability and control under a great range of loading condition. The bony architecture of the femur, tibia and patella contribute to the stability of stifle joint, along with static and dynamic restraint of the ligaments, capsule and musculature crossing the joint (Simon *et al*, 2000). Since camel is mainly used as a draught animal in India and any affection of the stifle joint can affect the working efficiency of the animal. This can impose an economical set back to poor farmers.

Radiography is effective for the evaluation of bony structures, but the fact that a 3-dimensional structure is projected onto a 2-dimensional plate leads to the major disadvantage of a superimposition of bony structures and lack of differentiation of soft tissues (Kraft and Gavin, 2001; Latorre *et al*, 2006 and Park *et al*, 1987). Previously, the radiographic study on stifle joints has been performed on canine (Innes *et al*, 2004) and equine (Nickles and Sande, 1982; Prades *et al*, 1989 and Bindeus *et al*, 2002) with satisfactory results.

Computed tomography allows cross sectional imaging without bone and soft tissue overlap. Furthermore, three-dimensional rendering of the area of interest and multiplanar reformatting can yield better anatomic orientation of the area of interest and provide for more sensitive detection and characterisation of disease extension (Tucker and Sande, 2001 and Bienert and Stadler, 2006). The CT scan studies were performed on Canine (Sammi and Dyce, 2004), Ovine (Vandeweerd *et al*, 2012) and Equine (Vekens *et al*, 2011) but such studies of the camel stifle joint had not yet been reported previously. Therefore, computed radiography and computed tomographic scanning of normal stifle joint of camel obtained from cadaver were studied and compared.

Materials and Methods

The present study was done on normal stifle joints taken from cadaver of adult camel. The stifle joint was studied radiographically by using Computed Radiography machine (Konica- Minolta computed radiographer, laser imager/printer Dry Pro∑ and Analyser/Reader Regius ∑II). The radiographs were taken with Allengers-525 (capacity 500 mA 300 KV). Lateral, cranio-caudal (Cr-Cd) and caudo-cranial (Cd-Cr) views were taken. Factors taken for lateral radiograph were 30 mAs and 80 kVp while for cranio-caudal (Cr-Cd) and caudo-cranial (Cd-Cr) view 35 mAs and 90 kVp.

The CT scan was done in a locally available medical lab equipped with CT scan facilities.The scan was taken with Wipro-GE Prospeed II CT Scanner. It was a spinning or commonly called as spiral CT

SEND REPRINT REQUEST TO AMIT SANGWAN email: 90amitsangwan@gmail.com

scan where entire X-ray tube spun around the central axis of the body part being scanned. The acquisition protocol was 120 kV and 130 mA. Image slices of 5 mm thickness were taken and reconstructed to study the stifle joint in 3 views i.e. 3-D, transverse and sagittal section. All important anatomical structures were identified and marked.

Results

Computed Radiography

Lateral View (Fig 1a):

The lateral computed radiography revealed femoro-tibial as well as femoro-patellar articulation. The femorotibial articulation was between convex femoral and concave tibial articular surfaces of respective sides. The lateral and medial menisci act as cushions between the respective articular surfaces of femur and tibia. The femoro-patellar articulation was between femoral trochlear groove and concave articular surface of patella. The patella appeared to be longer than wider. The anterior tibial tuberosity appeared clearly. There appeared a sharp depression just distal to the tuberosity.

Cranio-Caudal View (Fig 1b):

The articular surfaces of femur and tibia were clearly visible with a considerable gap between them. The patella was not distantly visible and femoral trochlea being covered by the patella could not be visible as well. The inter condylar tibial tubercles were visible, medial appeared some what larger

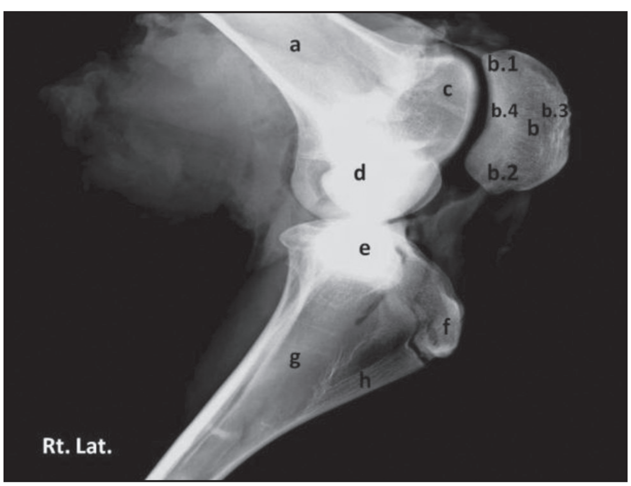

Fig (1a) Computed radiograph of right stifle joint lateral view. (a) Femur, (b) Patella, (b.1) Base of patella, (b.2) Apex of patella (b.3) Cranial rough surface of patella, (b.4) Smooth articular surface of patella, (c) Trochlea of femur, (d) Femoral condyle, (e) Tibial condyle, (f) Tibial tuberoity, (g) Tibia, (h) *Margo cranialis.*

and elevated than lateral. Both menisci (lateral and medial) were also visible.

Caudo-Cranial View (Fig 1c):

The caudo-cranial view clearly revealed the posterior articular surfaces of distal femur i.e. femoral condyles (medial and lateral) and proximal tibia

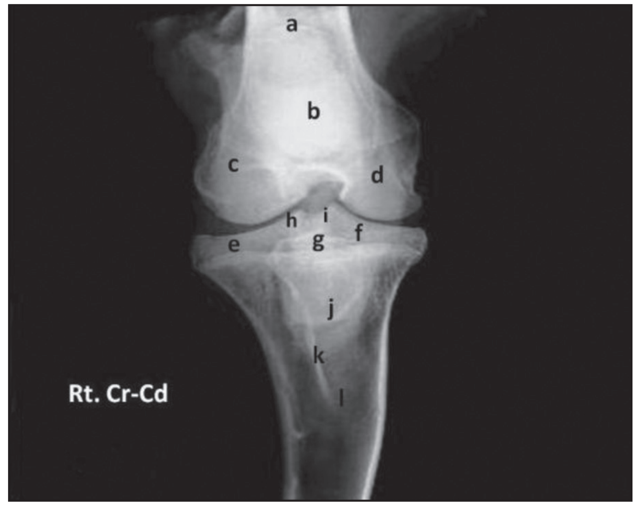

Fig (1b) Computed radiograph of right stifle joint cranio-caudal (Cr-Cd) view.
(a) Femur, (b) Patella, (c) Lateral condyle of femur, (d) Medial condyle of femur, (e) Lateral condyle of tibia, (f) Medial condyle of tibia, (g) Cranial intercondylar area, (h) Lateral intercondylar tubercle, (i) Medial intercondylar tubercle, (j) Tibial tuberosity, (k) *Margo cranialis,* (l) Tibia.

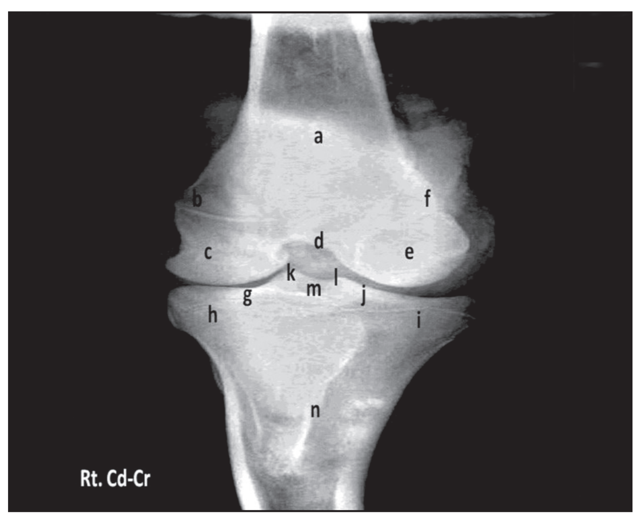

Fig (1c) Computed radiograph of right stifle joint joint caudo-cranial (Cd-Cr) view.
(a) Femur, (b) Medial epicondyle, (c) Medial condyle of femur, (d) Intercondylar fossa of femur, (e) Lateral condyle of femur, (f) Lateral epicondyle,(g) Medial meniscus, (h) Medial condyle of tibia, (i) Lateral condyle of tibia, (j) Lateral meniscus, (k) Medial intercondylar tubercle, (l) Lateral intercondylar tubercle, (m) Cranial intercondylar area, (n) Tibia.

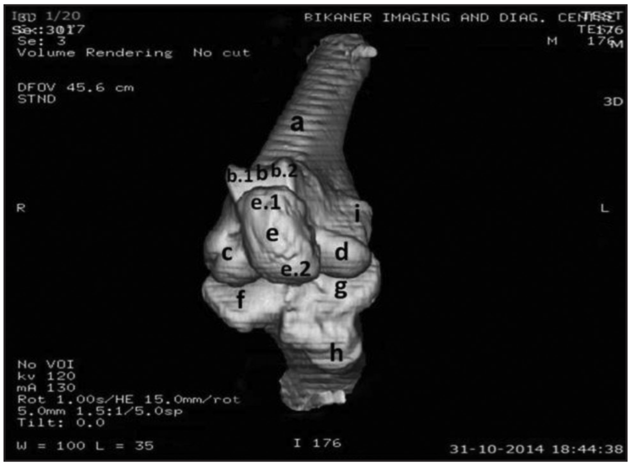

Fig (2a 1) 3-D CT scan image of right stifle joint showing cranial View.
(a) Femur, (b) Trochlea (proximal), (b.1) Lateral trochlear ridge, (b.2) Medial trochlear ridge, (c) Lateral condyle of femur, (d) Medial condyle of femur, (e) Patella, (e.1) Base of patella (e.2) Apex of patella (f) Lateral condyle of tibia, (g) Medial condyle of tibia, (h) Tibial tuberosity, (i) Medial epicondyle.

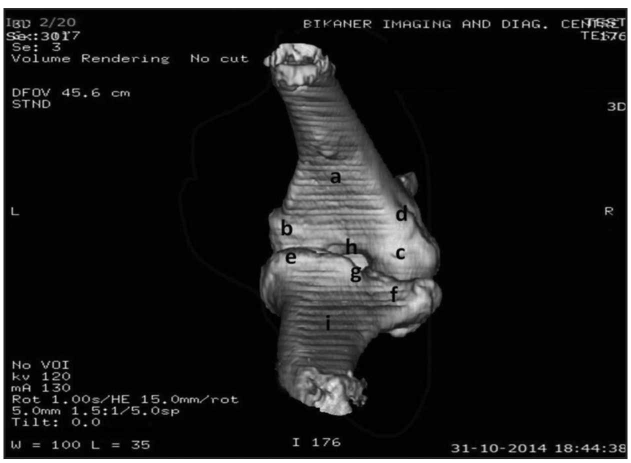

Fig (2a 2) 3-D CT scan image of right stifle joint showing caudal View.
(a) Femur, (b) Medial condyle of femur, (c) Lateral condyle of femur, (d) Lateral epicondyle of femur, (e) Lateral condyle of tibia, (f) Medial condyle of tibia, (g) Caudal intercondylar area of tibia, (h) Intercondylar fossa (femur), (i) Tibia.

(medial and lateral tibial condyles). The intercondylar tubercles were distinguishable and the intercondylar area was visible.

Computed Tomography Scan

The computed tomography scan was found advanced and a better method to study the stifle joint as compared to the computed radiography. Reformatted CT images in the 3-D, transverse and sagittal plane were evaluated for surface bony structures as well as the deeper or intra articular

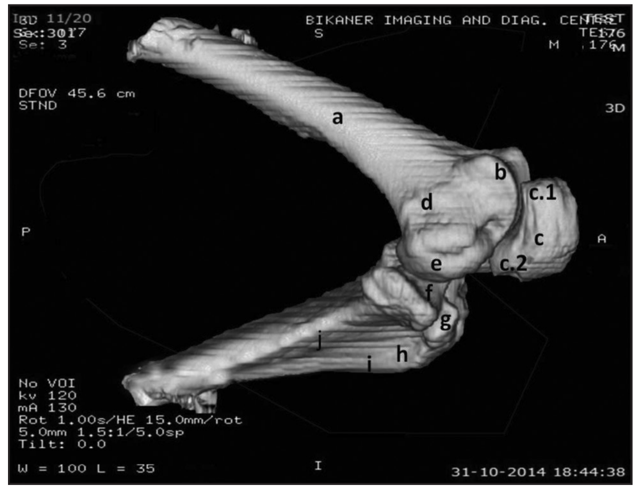

Fig (2a 3) 3-D CT scan image of right stifle joint showing lateral View.
(a) Femur, (b) Lateral trochlear ridge, (c) Patella, (c.1) Base of patella, (c.2) Apex of patella, (d) Lateral epicondyle, (e) Lateral condyle of femur, (f) Lateral condyle of tibia, (g) Lateral intercondylar tubercle, (h) Tibial tuberosity, (i) *Margo cranialis,* (j) Tibia.

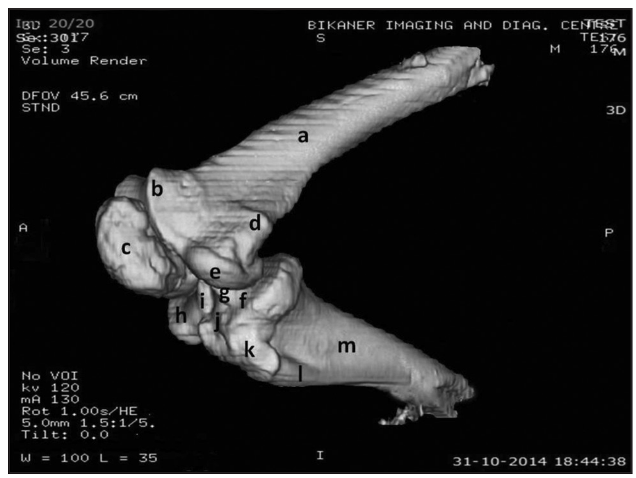

Fig (2a 4) 3-D CT scan image of right stifle joint showing medial View.
(a) Femur, (b) Trochlea, (c) Patella, (d) Medial epicondyle of femur, (e) Medial condyle of femur, (f) Medial condyle of tibia, (g) Medial intercondylar tubercle, (h) Lateral condyle of tibia, (i) Lateral intercondylar tubercle, (j) Cranial intercondylar area, (k) Tibialtu berosity, (l) *Margo cranialis,* (m) Tibia.

structures. The femur, tibia, and patella were clearly visible. The patellar ligaments, collateral ligaments and cranial and caudal cruciate ligaments could also be consistently evaluated. The cruciate ligaments and the menisco-tibial ligaments could be assessed in the sequences. Margins of the menisco-femoral ligament and the lateral and medial femoropatellar ligaments were difficult to visualise.

Stifle joint can be studied under following views of the joint:

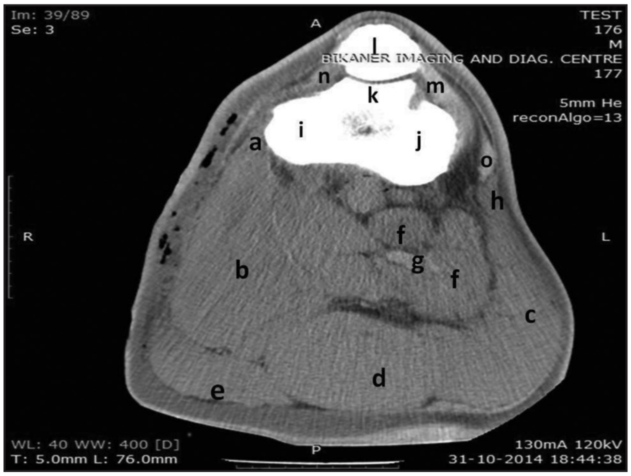

Fig (2b 1) Transverse CT scan image of right stifle joint. (a) Vastus lateralis, (b) Biceps femoris, (c) Gracilis, (d) Semimembranosus, (e) Semitendenosus, (f) Adductor, (g) Femoral vessels, (h) Sartorius, (i) Lateral condyle of femur, (j) Medial condyle of femur, (k) Trochlea, (l) Patella, (m) Medial femoropatellar ligament, (n) Lateral patellar retinaculum (o) Medial collateral ligament.

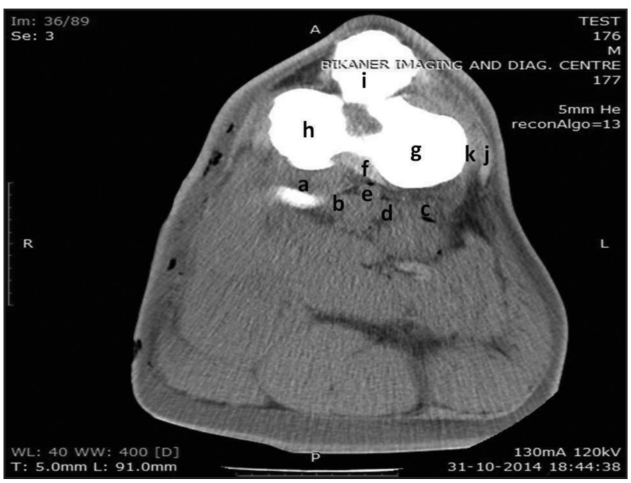

Fig (2b 2) Transverse CT scan image of right stifle joint. (a) Lateral meniscus, (b) Cranial attachment of lateral meniscus, (c) Medial meniscus (d) Cranial attachment of medial meniscus, (e) Cranial cruciate ligament, (f) Caudal cruciate ligament, (g) Medial condyle of femur,(h) Lateral condyle of femur, (i) Lateral condyle of femur, (j) Medial collateral ligament, (k) Attachment of medial meniscus to medial epicondyle.

3-D View (Figs 2a 1 to 2a 4):

The 3 dimensional view of stifle joint revealed the bony structures of the joint. Cranially the proximal femoral trochlea was seen while rest was covered by the patella (fig 2a 1). The femoral trochlear groove, medial and lateral ridges were clearly visible (fig 2a 1). As the joint specimen was kept in a flexed position the lateral and medial femoral condyles were clearly visible in cranial view. The cranial surface of the patella was rough. The medial aspect

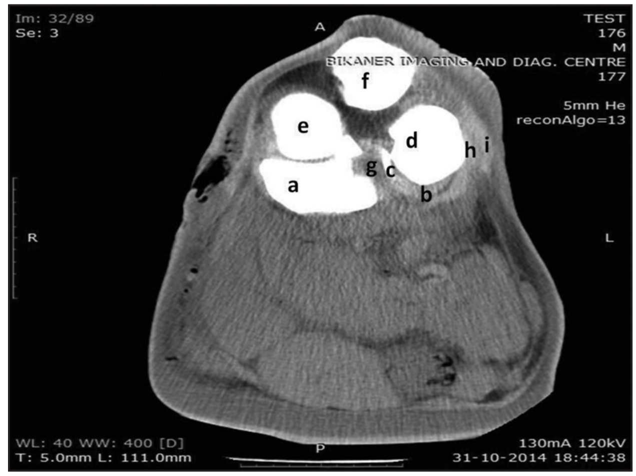

Fig (2b 3) Transverse CT scan image of right stifle joint. (a) Lateral condyle of tibia, (b) Medial meniscus, (c) Medial condyle of tibia, (d) Medial condyle of femur, (e) Lateral condyle of femur, (f) Patella, (g) Cranial intercondylar area, (h) Cranial attachment of medial meniscus, (i) Medial collateral ligament.

Fig (2b 4) Transverse CT scan image of right joint. (a) Deep digital flexor, (b) Superficial digital flexor, (c) Lateral digital extensor, (d) popliteus, (e) Gastrocnemius (lateral head), (f) Gastrocnemius (medial head), (g) Biceps, (h) Lateral condyle of tibia, (i) Lateral intercondylar tubercle, (j) Medial intercondylar tubercle, (k) Medial condyle of tibia.

of cranial surface of patella was smooth (Fig 2a 4) as compared to the lateral surface (fig 2a 3). Cranial intercondylar area of tibia could be seen. Caudally, the lateral and medial condyles and epicondyles of femur along with the respective condyles of tibia were evident (Fig 2a 4). The intercondylar fossa between femoral condyles was also evident caudally (Fig 2a 2). The tibial condyles (lateral and medial) were clearly visible articulating with the respective femoral condyles (Figs 2a 1, 2a 3 and 2a 4). The lateral

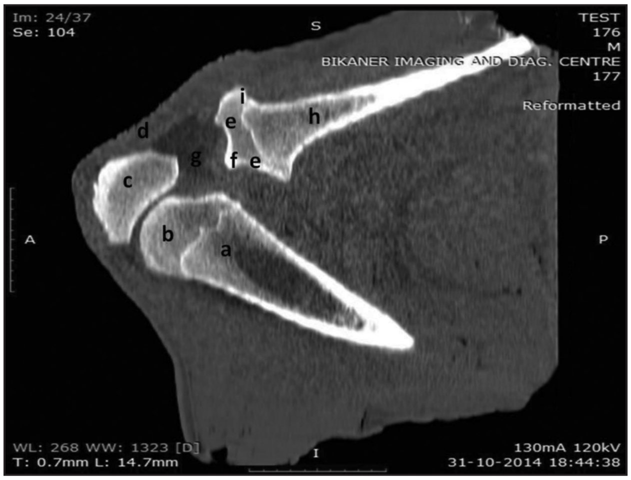

Fig (2c 1) Sagittal CT scan image of right stifle joint. (a) Femur, (b) Trochlea, (c) Patella, (d) Middle patellar ligament, (e) Tibial condyle, (f) Intercondylar tubercle, (g) Joint cavity, (h) Tibial tuberosity, (i) Tibia.

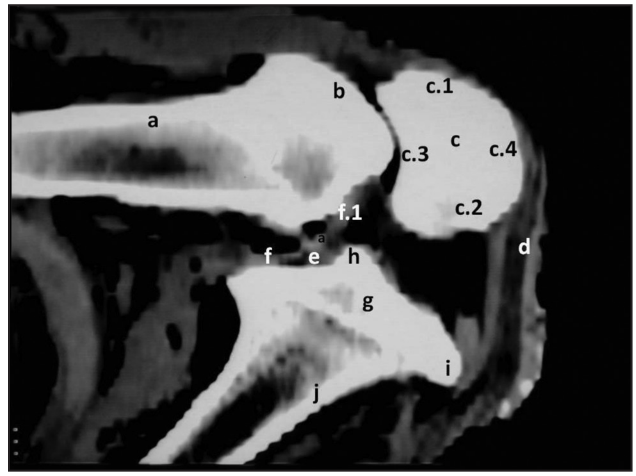

Fig (2c 2) Sagittal CT scan image of right stifle joint. (a) Femur, (b) Trochlea, (c) Patella, (c.1) Base of patella. (c.2) Apex of patella, (c.3) Smooth articular surface. (c.4) Rough anterior surface (d) Middle patellar ligament, (e) Cranial cruciate ligament, (f andf.1) Caudal cruciate ligament, (g) Tibial condyle, (h) Intercondylar tubercle, (i) Tibial tuberosity, (j) Tibia.

and medial intercondylar tibial tubercles were visible from lateral (Fig 2a 3) and medial (Fig 2a 4) views, respectively. The tibial tuberosity and *Margo cranialis* were clearly visible (Figs 2a 1, 2a 3 and 2a 4).

Transverse section (Figs 2b 1-2b 4):

As the whole joint could not be studied in single transverse section slice, they were evaluated sequentially. Transverse slices of the joint showed the bones as well as the ligaments. The femoral condyles, trochlea, the patella, tibialcondyles and menisci were distinguishable (Figs 2b 1, 2b 2 and 2b 4). The cranial intercondylar area of tibia was evidenced (Fig 2b 3). The intercondylar tibial tubercles (medial and lateral) could be evidenced (Fig 2b 4). The intraarticular ligaments like cranial and caudal cruciate ligaments (Fig 2b 2), medial collateral ligament (Figs 2b 1, 2b 2 and 2b 3), cranial attachments of medial and lateral menisci (Fig 2b 2) and attachment of medial meniscus to the medial epicondyle (Fig 2b 3) were distinguishable. The lateral patellar retinaculum could be evidenced (Fig 2b 1). The lateral collateral ligament was absent. The muscles associated with the stifle joint, distal femur and tibia were distinguishable (Figs 2b 1 and 2b 4).

Sagittal section (Figs 2c 1-2 c2):

The sagittal sections showed the whole joint i.e. the bones involved, the articular surfaces and the associated ligaments.

Discussion

The findings of computed radiography and computed tomography study of camel stifle joint were found to be mutually correlated and supportive. The lateral computed radiography revealed femorotibial as well as femoropatellar articulation. The patella appeared to be longer than wider. The patella was elongated with blunt base and pointed apex (apex directed distally). It was nearly congruent and articulate with femoral trochlea. The anterior tibial tuberosity appeared clearly. There appeared a sharp depression just distal to the tuberosity. These findings were in consonance with the gross anatomical findings of Smuts and Bezuidenhout (1987), Goldblatt and Richmond (2003), Dweek and Chung (2008), Siddiqui and Telfah (2010) and Fahmy *et al* (2011). The cranio-caudal and caudo-cranial radiographs revealed only femorotibial articulation as the patella covered the femoropatellar joint in the former view. Soft tissue structures could not be evidenced from computed radiography.

The computed tomography scan was found advanced and a better method to study the stifle joint as compared to the computed radiography as soft and bony tissues can be identifiable. Reformatted CT images in the 3-D, transverse and sagittal planes were evaluated for surface bony structures as well as the deeper or intra articular structures. The femur, tibia, and patella were clearly visible. The patellar ligaments, collateral ligaments and cranial and caudal cruciate ligaments could also be consistently evaluated.

Dhablania *et al* (1971) reported medial patellar desmotomy as a successful treatment of upward fixation of patella. In present study medial patellar ligament could not be evidenced as reported earlier by Krishnamurthy *et al* (1979), Smuts and Bezuidenhout (1987), Al-Ani (2004) and Siddiqui and Telfah (2010). The cruciate ligaments and the meniscotibial ligaments could be assessed in the sequences.

Manefield and Tinson (1997) stated that upward fixation of patella in camel denoted a tendency for the well developed fibrocartilage hook on the patella border to be caught on the medial trochlear proturbence. No such hook was evidenced in this study.

The incidence of hind limb lameness (54.68%) is more as compared to forelimb lameness (45.31%) in camel. Moreover, the upward fixation of patella is the 3rd most common (10.71%) cause of hind limb lameness (Gahlot, 2007). The most commonly described stifle joint affections are Gonitis and upward fixation of patella (Vaughan, 1965 and Wheat, 1972). The later is the most prevalent stifle affection in camel (Krishnamurthy *et al*, 1992). Other affections of stifle joint include the rupture of cruciate ligament (Purohit *et al*, 1988a; Pearce and Hurtig,1999 and Marriott *et al*, 1999), fibrotic myopathy of thigh muscles affecting the movement of the stifle joint (Purohit *et al*, 1988b), arthritis of stifle joint i.e. gonitis (Gahlot, 2000) and poisioning of *Capparis tomentosa*, a medicinal plant leading to stiffness of stifle joint (Schwartz and Dioli, 1992) etc. Classical anatomic atlases could not provide the spectrum of views and the details required in modern diagnostic and surgical techniques (Gehrmann *et al*, 2006; Dyson and Murray, 2007; Raji *et al*, 2008 and Vanderperren *et al*, 2008). Thus, present study may contribute significantly to the future research and diagnosis.

Conclusions

The stifle joint was a compound synovial joint having femoro-tibial (condylar joint) and femoro-patellar (sellar joint) articulation. The medial patellar ligament was not evidenced but medial femoropatellar ligament could be evidenced. Among collateral ligaments only medial was evidenced. The CT scan of camel stifle joint was found valuable in revealing the bony as well as soft tissues and thus was considered a step ahead than computed radiography. Such findings might be important as a reference of normal joint and helpful in diagnosis of surgical affections or anatomical defects of joint.

References

Al-Ani (2004). Camel Management and Diseases. 1st Edition. Dar Ammar Book Publisher. pp 319.

Bindeus T, Vrba S, Gabler C, Rand T and Stanek C (2002). Comparison of computed radiography and conventional film-screen radiography of the equine stifle. Veterinary Radiology and Ultrasound 43(5):455-60.

Bienert A and Stadler P (2006). Computed tomographic examination of the locomotor apparatus of horses – a review. Pferdeheilk 22:218–222.

Dhablania DC, Tyagi RPS and Vig MM (1971). Stringhalt in camels a case report. Indian Veterinary Journal 48(5):416-419.

Dweek J and Chung C (2008). The patellar extensor apparatus of the knee. Pediatric Radiology 38:925-935.

Dyson S and Murray R (2007). Magnetic resonance and imaging of equine fetlock. Clinical Techniques in Equine Practice 6(1):62-77.

Fahmy LS, Mostafa MB, Faray KA and Hegazy AA (2011). Arthrographic evaluation of the stifle joint in the camel (*Camelus dromedarius*). In: Selected Research on Gross Anatomy and Histology of Camels. Gahlot TK, Saber AS, Nagpal SK and Jianli W. 1st edition. Camel Publishing House. pp 41-43.

Gahlot TK (2000). Selected Topics on Camelids. The Camelid Publishers. 1st Edition. pp 424.

Gahlot TK (2007). Lameness in camels. In: Proceedings of the International Camel Conference "Recent Trends in Camelids Research and Future Strategies for Saving Camels", Rajasthan, India. pp 158-167.

Gehramann S, Hohne KH, Linhart W, Pflessor B, Pommert A, Riemer M, Tiede U, Windoff J, Schumacher J and Rueger JM (2006). A novel interactive anatomic atalas of hand. Clinical Anatomy 19:258-66.

Goldblatt J and Richmond J (2003). Anatomy and biomechanics of the knee. Operative Technique in Sports Medicine 11:172-186.

Innes JF, Costello M, Barr FJ, Rudorf H and Barr ARS (2004). Radiographic Progression of Osteoarthritis of the Canine Stifle Joint: A Prospective Study. Veterinary Radiology and Ultrasound 45(2):143-148.

Kraft SL and Gavin P (2001). Physical principles and technical considerations for equine computed tomography and magnetic resonance imaging. Veterinary Clinics of North America: Equine Practice 17:115-30.

Krishnamurthy D, Tyagi RPS and Sharma DN (1979). Absence of medial patellar ligament in camels. Indian Veterinary Journal 56:243-245.

Krishnamurthy D, Tyagi RPS and Sharma DN (1992). Upward fixation of patella in camels. In: Proceedings of 1st International Camel Conference, Dubai. pp:357-359.

Latorre R, Arencibia A, Gil F, Rivero M, Henry RW, Ramirez G and Vaquez JM (2006). Correlation of magnetic resonance images with anatomic features of the equine tarsus. American Journal of Veterinary Research 67:756-761.

Manefield GW and Tinson AH (1997). Camels a compandium. University of Sydney Post Graduate Foundation in Veterinary Science. 22 (c) pp 139-140.

Marriott MR, Dart AJ, Macpherson C and Hodgson DR (1999). Repair of cranial cruciate ligament rupture in an alpaca. Australian Veterinary Journal 77:654-55.

Nickels FA and Sande R (1982). Radiographic and Arthroscopic findings in the equine stifle. Journal of American Veterinary Medical Association 181(9):918-24.

Pearce SG and Hurtig MB (1999). Surgical repair of a ruptured cranial cruciate ligament in a dromedary camel. Journal of American Veterinary Medical Association 215(19):1325-7.

Park RD, Nelson TR, Hoopes J (1987). Magnetic resonance imaging of the normal equine digit and metacarpophalangeal joint. Veterinary Radiology 28:105-16.

Prades M, Grant BD, Turner TA, Nixon AJ and Brown MP (1989). Injuries to the cranial cruciate ligament and associated structures: summary of clinical, radiographic, arthroscopic and pathological findings from 10 horses. Equine Veterinary Journal 21(5):354-357.

Purohit NR, Chauhan DS, Chaudhary RJ, Dudi PR and Deora KS (1988a). Rupture of cruciate ligament of Stifle Joint. Indian Journal of Veterinary Surgery 9(2):139-140.

Purohit NR, Chauhan DS, Chaudhary RJ, Dudi PR and Deora KS (1988b). Unusual fibrotic myopathy. Indian Journal of Veterinary Surgery 9(2):136-137.

Raji AR, Sardari K and Mohammadi HR (2008). Normal cross sectional anatomy of bovine digit: comparision of computed tomography and limb anatomy. Anatomia Histologia Embryologia 37:188-91.

Samii VF and Dyce J (2004). Computed tomographic arthrography of the normal canine stifle. Veterinary Radiology and Ultrasound 45(5):402-6.

Schwartz HJ and Dioli M (1992). The One Humped Camel in Eastern Africa: A Pictorial Guide to Diseases, Health Care and Management. Verlag Josef Margeaf Scientific Books. pp 220-221.

Siddiqui MI and Telfah MN (2010). A Guide Book of Camel Surgery. Abu Dhabi Food Control Authority (ADFCA). pp 147-148.

Simon SR, Einhorn TA and Buckwalter JA (2000). Kinesiology. In: Orthopaedic basic science: Biology and Biomechanics of the musculoskeletal system. 2nd edition. American Academy of Orthopaedic Surgery. pp 730-827.

Smuts MMS and Bezuidenhout AJ (1987). Anatomy of the Dromedary. Oxford Science Publications. pp 54-56.

Tucker RL and Sande RD (2001). Computed tomography and magnetic resonance imaging of the equine musculoskeletal conditions. Veterinary Clinics of North America: Equine Practice 17:145–157.

Vanderperan K, Ghaye B, Hoegaerts M and Saunders JH (2008). Evaluation of the computed tomographic anatomy of Equine Metacarpophalangeal Joint. American Journal of Veterinary Research 69:631-8.

Vandeweerd JM, Kirschvink N, Muylkens B, Depiereux E, Clegg P, Herteman N, Lamberts M, Bonnet P and Nisolle JF (2012). A study of the anatomy and injection techniques of the ovine stifle by positive contrast arthrography, computed tomography arthrography and gross anatomical dissection. The Veterinary Journal 193:426-432.

Vaughan JT (1965). Analysis of lameness in pelvic limb and selected cases. In: Proceedings of 11th Annual Convention. American Association of Equine Practice. pp 223-241.

Vekens EV, Bergman EH, Vanderperren K, Raes EV, Puchalski SM, Bree HJ and Saunders JH (2011). Computed Tomographic anatomy of equine stifle joint. American Journal of Veterinary Research 72(4):512-21.

Wheat JD (1972). Conditions of hind limb and lower back. In: Equine Medicine and Surgery. 2nd edition. Eds. Catcott EJ and Smith JF. American Veterinary Publication Inc. pp 563-574.